

## Red light-emitting diodes based on InP/GaP quantum dots

F. Hatami,<sup>a)</sup> V. Lordi, and J. S. Harris

*Department of Electrical Engineering, Stanford University, Stanford, California 94305*

H. Kostial

*Paul-Drude Institut für Festkörperelektronik, Hausvogteiplatz 5-7, 10117 Berlin, Germany*

W. T. Masselink

*Department of Physics, Humboldt Universität zu Berlin, Newtonstrasse 15, 12489 Berlin, Germany*

(Received 19 July 2004; accepted 8 February 2005; published online 21 April 2005)

The growth, fabrication, and device characterization of InP quantum-dot light-emitting diodes based on GaP are described and discussed. The diode structures are grown on gallium phosphide substrates using gas-source molecular-beam epitaxy and the active region of the diode consists of self-assembled InP quantum dots embedded in a GaP matrix. Red electroluminescence originating from direct band-gap emission from the InP quantum dots is observed at low temperatures. With increasing temperature, however, the emission line shifts to the longer wavelength. The emission light is measured to above room temperature. © 2005 American Institute of Physics. [DOI: 10.1063/1.1884752]

Light-emitting semiconductor devices are key components for information transmission, information storage, visible displays, and lighting. Today, GaP is usually used for emission in wavelengths sensitive to human vision from red to green.

GaP, however, is an indirect band-gap semiconductor with a low luminescence efficiency because of the different crystal momentum of electrons and holes. Useful light emission is made possible by doping the GaP with deep levels. The resulting spatial localization of electrons at such deep levels leads to a delocalization in momentum space and therefore to components of the electron wave function having the same crystal momentum as the holes.<sup>1</sup> For many applications, however, light-emitting diodes (LEDs) with a higher emission efficiency are required. Direct band-gap InP quantum dots (QDs) embedded in a GaP matrix and on a GaP substrate offer a promising solution to these challenges. First, using different sizes of QDs allows to change the emission light between orange and red.<sup>2</sup> Second, the use of GaP as substrate takes advantage of a well-established LEDs technology. Third, using the transparent GaP as a substrate, compared to the other commercial LEDs based on GaAs and AlGaAs, allows easier extraction of the emitted light for vertical structures such as superluminescent LEDs or vertical cavity lasers. Finally, in contrast with AlGaInP and AlGaAs LEDs,<sup>3</sup> the advantage of InP QDs is that the structures are realized during a simple epitaxial process. Hence, several fabrication steps such as wafer bonding can be reduced.

The most extensively investigated QD system is InAs/GaAs. Band-to-band and intersubband lasers based on InAs/GaAs QDs have been demonstrated by several groups [see, for example, (Refs. 4–6)]. InP/GaP QDs have been much less extensively investigated than InAs/GaAs QDs. Recently, we have demonstrated photoluminescence from InP QDs embedded in GaP matrix on GaP substrate.<sup>2,7</sup> These

QDs were furthermore shown to be direct band gap with type-I heterointerfaces.<sup>7,8</sup> In this letter we describe the growth, fabrication, and characterization of LEDs based on InP QDs within a GaP matrix and on a GaP substrate.

Samples are grown using gas-source molecular-beam epitaxy (GSMBE) on (001)-GaP:S substrates in a RIBER-32-P MBE system. After oxide desorption, a 200-nm silicon-doped GaP buffer layer ( $n \approx 5 \times 10^{17} \text{ cm}^{-3}$ ) is grown at 530 °C at a rate of 0.94  $\mu\text{m/h}$  and under 3 SCCM (standard cubic centimeter per minute)  $\text{PH}_3$  flux. After a short growth interruption to lower the substrate temperature, between three and five monolayers (ML) of InP are deposited at 510 °C at a rate of 0.27  $\mu\text{m/h}$ . Immediately after the InP deposition, the structure is annealed for 60 s, followed by the growth of a 3-nm GaP again at 510 °C. This procedure is repeated three times. The substrate temperature is then increased to 530 °C for the growth of a 700-nm beryllium-doped GaP ( $p \approx 5 \times 10^{17} \text{ cm}^{-3}$ ). The resulting sequence is capped with a 10-nm beryllium-doped GaP ( $p \approx 1 \times 10^{19} \text{ cm}^{-3}$ ). The growth process is monitored using reflection high-energy electron diffraction (RHEED); during GaP growth, the surface shows a  $(2 \times 4)$  reconstruction. At the beginning of InP growth, the RHEED pattern appears streaky, indicating a two-dimensional growth. After deposition of about 2-ML InP, however, the large lattice mismatch between InP and GaP of about 7.7% results in the formation of Stranski-Krastanow InP QDs and RHEED pattern gradually becomes spotty and less intense.

After growth, the structures are fabricated into LEDs for electroluminescence (EL) measurements. First a 150-nm-thick layer of Au:Ge (99.5:0.5) is deposited on the back side by thermal evaporation. The top-ring contacts are made from Au:Be (99:1) and are prepared using lift-off technology. The contacts are 150 nm thick with an outer diameter of about 50  $\mu\text{m}$ . Subsequently, the contacts are alloyed at 575 °C. Using photolithography, dots with a 230- $\mu\text{m}$  size for the mesa etching are defined on the top of

<sup>a)</sup>Electronic mail: hatami@physik.hu-berlin.de

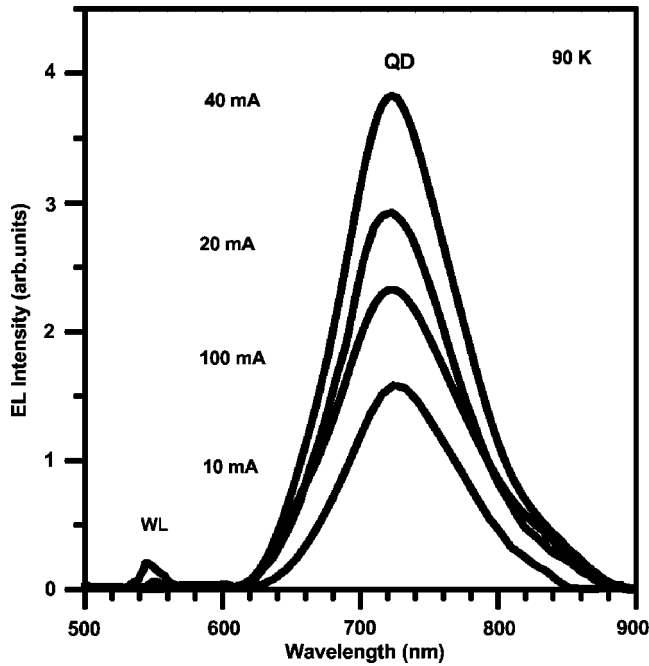


FIG. 1. Current dependence of the EL spectra at 90 K.

the ring contacts. The mesas are etched using reactive ion etching resulting in a mesa depth of 1150 nm and vertical sidewalls of the mesas.

The resulting devices are characterized using the EL measurements carried out in a liquid-helium cryostat in the temperature range of 70–300 K. A HP 3458A multimeter is used for supplying the power and a Keithley SMU 236 multimeter measured the current. The emitted light is dispersed by a 1-m monochromator and detected by a charge-coupled device camera. Some EL measurements use an ILX Lightwave LDC-3722 current source modulated by a square-wave pulse generated by a HP 33120A function generator and the emission light is dispersed by a 0.3-m monochromator and detected by a silicon detector using a lock-in technique.

The light output from the InP/GaP QDs LEDs consists of two lines peaked in the green and red ranges. The sharp green line having 20-nm full width at half maximum peaks at about 550 nm and appears to result from carrier recombination in the strained InP wetting layer and perhaps in the surrounding GaP matrix. The red line at about 720 nm is attributed to electron-hole recombination in the quantum dots. For currents lower than 100 mA, the electroluminescence spectra are dominated by the red EL line due to the QDs.

The current dependence of the EL spectra at 90 K is shown in Figs. 1 and 2. As the current is increased from 1 to about 45 mA, the integrated QD electroluminescence intensity grows by a factor of 9 and does not significantly change for currents between 45 and 60 mA. For currents lower than 30 mA, the intensity grows sublinearly. The EL intensity generally decreases for currents higher than 60 mA. Similar dependence of EL intensity on current is also observed for the other temperatures and will be discussed later. The current for which the maximum EL intensity is obtained,  $I_{\max}$ , however, depends on the temperature, shifting to higher cur-

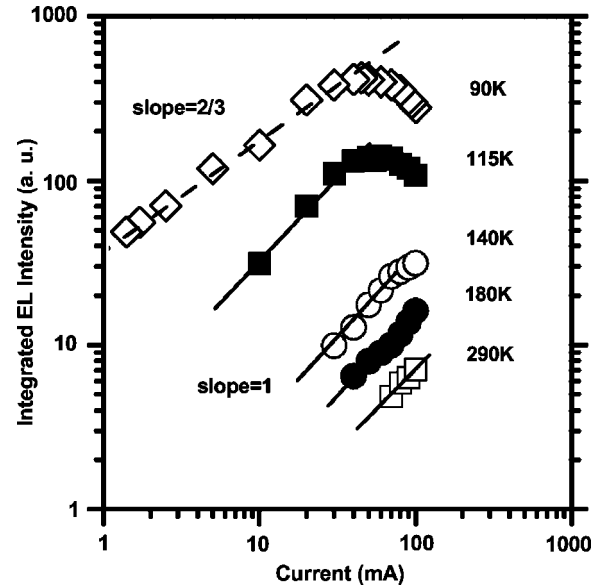


FIG. 2. Current dependence of the integrated EL intensity for several temperatures. The dashed and solid lines show slopes of 2/3 and 1, respectively.

rent values for higher temperatures. At 140 K the maximum EL intensity is achieved at 95 mA and for higher temperatures  $I_{\max}$  is more than 100 mA.

Under the conditions of Boltzmann statistics and an absence of leakage current, the injected current is given by the rate equation<sup>9</sup>

$$I = An + Bn^2 + Cn^3, \quad (1)$$

where  $n$  denotes the injected carrier density and  $An$ ,  $Bn^2$ , and  $Cn^3$  are the current components originating from nonradiative recombination, radiative recombination, and Auger recombination, respectively. The constants  $A$ ,  $B$ , and  $C$  are temperature dependent. In Auger recombination, three carriers are involved and the energy of recombination of two of them is given to the third carrier. The Auger coefficient  $C$  increases slightly with increasing carrier density.<sup>10,11</sup> The light output  $P$  is proportional to the radiative recombination ( $P \propto n^2$ ). If we express the injected carrier density as  $I \propto n^z$ , the differential efficiency  $\eta$  is proportional to  $I^{2/z}$ . Thus, the dependence of  $\eta$  on  $n$  through the parameter  $z$  provides insight into the emission.

Figure 2 shows the integrated electroluminescence intensity of the QD emission as a function of current for several temperatures in a logarithmic plot. For low temperatures (<110 K) and lower current, the EL intensity grows sublinearly with an exponent of about 2/3 ( $z \approx 3$ ). For temperatures higher than 100 K, the intensity grows linearly ( $z \approx 2$ ) until saturation; for temperatures higher than 140 K, the saturation occurs at currents greater than 100 mA.

We explain the EL intensity behavior as follows: At low temperatures and for currents lower than 30 mA, the parameter  $z \approx 3$  is consistent with the dominant current contribution being Auger recombination. Apparently, the current in that range is sufficiently high for injection of a large number of carriers, most of which are captured by the QDs at low temperatures. At high carrier concentration in the QDs, Au-

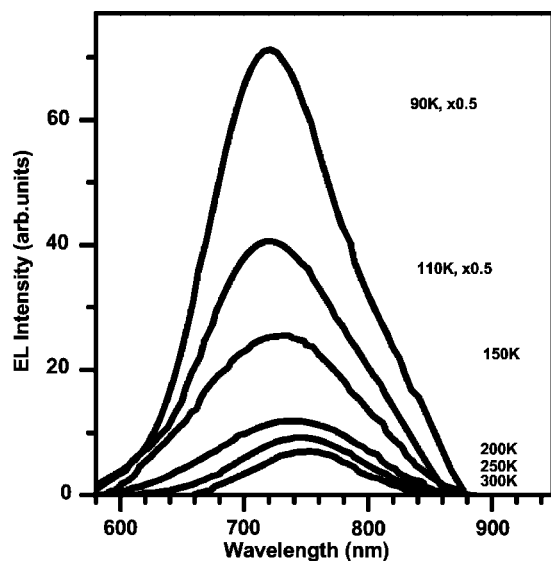


FIG. 3. Temperature evolution of the EL spectra under constant current of 100 mA.

ger recombination has been shown to be important.<sup>10,11</sup> A decrease of the Auger coefficient with increasing temperature for InGaAs/GaAs QDs has been recently reported.<sup>12</sup> With increasing temperature, the QDs capture fewer carriers and, hence, the carrier density in the QDs decreases. Consequently, the Auger process becomes weaker and the differential efficiency is proportional to  $z \approx 2$ , indicating that radiative recombination is the dominant recombination process. The same effect has been reported for Ge/Si QDs by Chang *et al.*<sup>13</sup> In contrast with an ideal *p-i-n* structure based on a quantum well and with linear light-current dependence, structures based on QDs exhibit saturation effects due to the limited number of QDs and the limited density of states in each QD. These saturation phenomena in QDs have been reported in several works.<sup>14,15</sup> Because quantum dots capture carriers more efficiently at low temperatures, the saturation occurs at lower injection currents. As the temperature increases, the QDs trap fewer carriers and, therefore, more injected carriers are needed for saturation, shifting  $I_{\max}$  to higher currents with increasing temperature. We propose that the decrease in EL intensity after the saturation of the QDs is due to heating and perhaps the band-filling effect in the QDs. As current increases, the temperature of the active region also increases, resulting in the thermal escape of carriers from the QDs and consequently a decrease in QD-related light output. At this point, this loss in the light output is more significant than its increase due to the increased injection current density through the junction. Note that for currents lower than 100 mA, the red EL intensity from the QDs is at least 60 times greater than the EL intensity originating from the wetting layer.

For device applications, the characteristics of the electroluminescence near room temperature are of utmost importance. Figure 3 shows the temperature evolution of EL spec-

tra with a constant injection current of 100 mA. As the temperature is increased from 70 to 300 K, the EL peak maximum shifts from 720 to 752 nm. This redshift follows the temperature dependence of the band gap of InP bulk with about 300-meV offset. We point out that the electroluminescence from QDs is observed to above room temperature and the EL intensity decreases only by a factor of 60 as the temperature is raised from 70 K to room temperature.

The external quantum efficiency  $\eta_{\text{ex}}$  is estimated using the measured light output power versus injection current. At 70 K  $\eta_{\text{ex}}$  is about 1.3%. It should be noted, however, that the investigated samples are not packaged and it is quite difficult to measure absolute efficiency of spontaneous emission, especially when the sample is mounted in a cryostat. Hence, 1.3% is the lower limit of the estimated quantum efficiency of QDs.

To conclude, we have demonstrated and investigated LEDs based on self-assembled InP quantum dots in a GaP matrix on a GaP substrate. The QDs are grown using gas-source MBE in the intrinsic region of *p-i-n* diodes and show red electroluminescence peaking at about 720 nm at low temperature. The emission originates from direct band-gap, type-I heterointerfaces InP QDs. Achieving electroluminescence from indirect GaP by means of direct band-gap InP QDs offers a promising alternative to the part of currently used LEDs. Furthermore, they open the possibility for vertical light emitters, such as superluminescent LEDs or vertical cavity lasers based on GaP.

The authors thank G. Mussler for technical support. One of the authors (F.H.) acknowledges Alexander von Humboldt foundation for supporting her research at Stanford as Feodor-Lynen fellow. Another author (V.L.) acknowledges the Fannie and John Hertz foundation for financial support.

<sup>1</sup>W. T. Masselink and Y.-C. Chang, Phys. Rev. Lett. **51**, 509 (1983).

<sup>2</sup>F. Hatami, L. Schrottke, and W. T. Masselink, Appl. Phys. Lett. **78**, 2163 (2001).

<sup>3</sup>Th. Gessmann and E. F. Schubert, J. Appl. Phys. **95**, 2203 (2004).

<sup>4</sup>K. Kamath, P. Bhattacharya, T. Sosnowski, T. Norris, and J. Phillips, Electron. Lett. **32**, 1374 (1996).

<sup>5</sup>D. L. Huffaker, G. Park, Z. Zou, O. B. Shchekin, and D. G. Deppe, Appl. Phys. Lett. **73**, 2564 (1998).

<sup>6</sup>N. Kirstaedter *et al.*, Appl. Phys. Lett. **69**, 1226 (1996).

<sup>7</sup>F. Hatami, W. T. Masselink, L. Schrottke, J. W. Tamm, V. Talalaev, C. Kristukat, and A. R. Göni, Phys. Rev. B **67**, 085306 (2003).

<sup>8</sup>A. R. Göni, C. Kristukat, F. Hatami, S. Dreßler, W. T. Masselink, and C. Thomsen, Phys. Rev. B **67**, 075306 (2003).

<sup>9</sup>S. Hausser, G. Fuchs, A. Hangleiter, K. Streubel, and W. T. Tsang, Appl. Phys. Lett. **56**, 913 (1990).

<sup>10</sup>W. Bardyszewski and D. Yevick, J. Appl. Phys. **58**, 2713 (1985).

<sup>11</sup>S. Picozzi, R. Asahi, C. B. Geller, and A. J. Freeman, Phys. Rev. Lett. **89**, 197601 (2002).

<sup>12</sup>S. Ghosh, P. Bhattacharya, E. Stoner, J. Singh, H. Jiang, S. Nuttinck, and J. Laskar, Appl. Phys. Lett. **79**, 722 (2001).

<sup>13</sup>W.-H. Chang *et al.*, Appl. Phys. Lett. **83**, 2958 (2003).

<sup>14</sup>R. Murray, D. Childs, S. Malik, P. Sivers, C. Roberts, J.-M. Hartmann, and P. Stavrinou, Jpn. J. Appl. Phys., Part 1 **38**, 528 (1999).

<sup>15</sup>J. X. Chen, U. Oesterle, A. Fiore, R. P. Stanley, M. Ilegems, and T. Todaro, Appl. Phys. Lett. **79**, 3681 (2001).